Korean J. Chem. Eng., 39(10), 2810-2816 (2022)
DOI: 10.1007/s11814-022-1108-1

pISSN: 0256-1115
eISSN: 1975-7220

Scrap oxidation of uranium carbide heavy ion accelerator target material

Bohyun Jo† **and Youngho Shim**

Kepco Nuclear Fuel Company, Daejeon 34057, Korea

(*Received 10 January 2022 • Revised 6 March 2022 • Accepted 14 March 2022*)

Abstract−The use of uranium carbide for extracting uranium, a rare and valuable material, has garnered significant research interest. The long-term storage of uranium scrap is challenging due to the risk of ignition and contents of nuclear materials. Thus, scrap treatment is required for safe storage and volume reduction. We investigated the oxidation behavior of different types of multi-walled carbon nanotube-containing uranium scraps (green and sintered) in different forms (fragmented and powdered) using thermogravimetric/differential thermal analysis and volatilization studies. An air flow and oxidation temperature of 500 cm^3/min and 900 °C, respectively, were suitable for the effective recovery of inert U_3O_8 for safe storage or recycling. For optimal results, scrap in powder form should be used. These findings provide insights for recycling uranium from uranium carbide scrap, with potential applications in research and industry.

Keywords: UC_2-C Scrap, Uranium Carbide, MWCNT, Scrap Oxidation, Heavy Ion Accelerator Target Material

INTRODUCTION

In the 1960s, uranium carbide (UC) gained popularity as a nuclear fuel owing to its high uranium density and thermal conductivity (25.3 W/(m·K)), which are higher than those of uranium oxide by factors of 1.34 and 2.6, respectively. However, the use of UC then decreased owing to its low oxidation resistance, and uranium oxide is currently one of the main components of nuclear fuels [1-5].

Recently, research on UC has re-emerged. Its potential as a nuclear fuel in fourth-generation nuclear reactors is attracting attention, and several researchers are focusing on UC as a heavy ion accelerator target material because of its high vapor pressure limiting temperature (2,100 °C), in addition to the advantages mentioned above [6-10]. The vapor pressure limiting temperature refers to the temperature at which the vapor pressure begins to adversely affect the ionization efficiency of the generated isotopes [11-13]. Nuclear fuel is composed purely of UC, and the heavy ion accelerator target typically comprises a dispersed mixture of a carbon source and UC_2 particles, denoted as UC_2-C. Multi-walled carbon nanotubes (MWCNTs) are widely used as the carbon sources, because they exhibit thermal conductivity superior to that of graphite, and their net-like structure securely traps the uniformly distributed UC_2 particles.

The heavy ion accelerator target is closely related to the isotope yield. An ideal target material should generate as many isotopes as possible, with short release times. In addition, it should exhibit good thermal conductivity to improve the heat dissipation, and a good permeability to improve the effusion of the generated isotopes. Therefore, the target material should exhibit a small UC_2 particle size (<0.5 μm), low density, and high porosity (70%). Thin disks (0.8-1.3 mm) with a large diameter (40-50 mm) are preferred [14-16].

However, fabricating such UC_2-C disks is challenging, and because of the high risk of ignition after fabrication, additional precautionary measures are required during handling. Thus, optimizing the conditions of the fabrication of the UC_2-C disks is critical in yielding acceptable target materials that satisfy quality standards. Generally, the target materials are fabricated by pulverizing uranium dioxide powder with a carbon source, followed by processing and reduction via heating under vacuum. Improper storage or handling may yield defective products, particularly owing to interactions with oxygen or moisture due to the risk of oxidation. Such defective products are discarded as waste or scrap. Waste materials cannot be utilized, whereas scrap materials may still be used after further treatment. The scrap is classified as green or sintered scrap, depending on whether it is produced before or after reduction via heating.

The long-term storage of uranium scrap is challenging due to the risk of ignition and contents of nuclear materials. Therefore, scrap treatment (uranium recovery) is required for safe storage and volume reduction. Moreover, because the CNTs in the scrap are nanosized particles, which may be toxic or carcinogenic to the human body, these should be removed via oxidation using gases [17-19].

Research regarding the mechanism of UC oxidation aims to convert it to inert U_3O_8 for safe storage or recycling. The oxidation mechanism is affected by the temperature, atmosphere, oxide layer thickness, stoichiometry, and treatment conditions [4,20-23]. Herein, we recovered uranium from scrap formed during the fabrication of UC as a heavy ion accelerator target by removing the MWCNTs by oxidation via heating. A temperature of >600 °C and an air flow of 500 cm^3/min were suitable for effective uranium recovery. This method of scrap oxidation is patented and registered in South Korea [24].

METHODS

1. Specimens

1-1. Scrap Material

The specified particle size of UC_2 on isotope separation on-line (ISOL) target materials is <0.5 μm for the operation of heavy ion

---

†To whom correspondence should be addressed.
E-mail: bhcho@knfc.co.kr

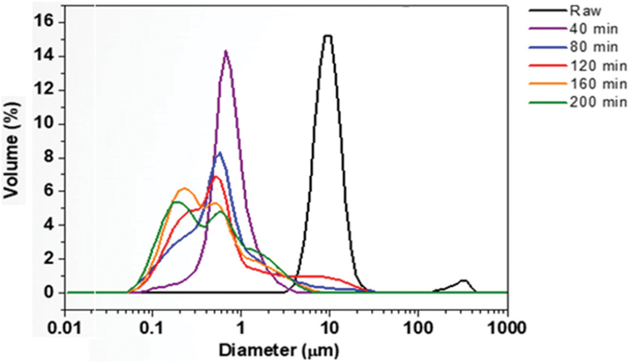

Fig. 1. Particle size distribution and the variation in U_3O_8.

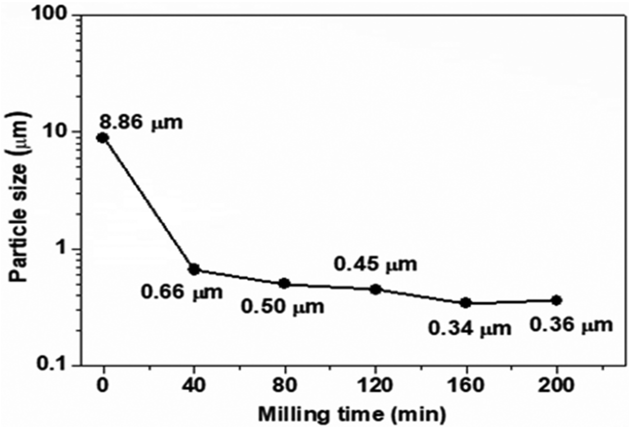

Fig. 2. U_3O_8 particle size with crushing time.

accelerators in the Republic of Korea to improve the emission efficiency of radioactive isotopes produced during proton irradiation. U_3O_8 is crushed using a planetary mill (PM 100, Retsch, Haan, Germany) at 500 rpm (5 min crushing, 3 min resting) for ~160 min to form a U_3O_8 powder of ~0.3 μm in size. Fig. 1 shows the particle size distribution and the variation in U_3O_8 and Fig. 2 shows U_3O_8 particle size with crushing time, which were obtained using specific surface area (ASAP 2460, Micromeritics, Norcross, GA, USA) and particle size (Partica LA-960, Horiba, Kyoto, Japan) analyzers.

Two types of starting materials were used in this study: green and sintered scraps. The green scrap (U_3O_8-C) was formed by finely mixing powdered U_3O_8 (70 wt%, 0.17 μm) with a carbon source (30 wt%), whereas the sintered scrap (UC_2-C) was formed via carbothermal reduction (1,800 °C, 2 h) of UC_2-C under vacuum ($<3\times 10^{-5}$ Torr). MWCNTs with excellent thermal conductivities and net-like structures were used as the carbon sources.

U_3O_8 is directly converted to UC_2 of 0.3 μm in size during carbothermal reduction without particle growth as U_3O_8 is uniformly dispersed within the parent MWCNT. U_3O_8 is converted to UC via the following chemical reactions.

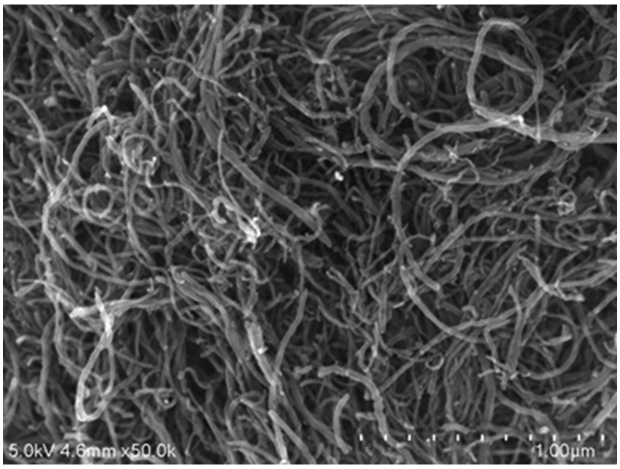

Fig. 3. MWCNT morphology.

Stage 1: $U_3O_8+28C \rightarrow 3UC_2+18C+4CO_2$ (600-700 °C)
Stage 2: $U_3O_8+20C \rightarrow 3UC_2+6C+8CO$ (1,250-2,000 °C)

Table 1 shows the specifications of the sintered scrap UC_2-C disks. Two types of sintered scrap specimens were prepared: fragmented and powdered. The powdered specimen was prepared via pulverization for 10 min using an agate mortar and pestle in a glove box under Ar gas.

1-2. MWCNTs

Fig. 3 shows a scanning electron microscopy (SEM; SU8230, Hitachi, Tokyo, Japan) image of the MWCNTs (Avention, Siheung-si, Republic of Korea). The MWCNTs exhibit external diameters of 5-15 nm and lengths of 0.5-2 μm. The MWCNT purity was >95 wt% CNTs, >97 wt% C, and <1.5 wt% ash.

2. Characterizations

The volatilization behavior of the MWCNTs and green and sintered scraps in air was observed using thermogravimetric/differential thermal analysis (TG-DTA; SETSYS Evolution, Setaram, Lyon, France) and volatilization studies in an electric furnace. For the TG-DTA studies, 30 mg samples were heated to 900 °C at 5 °C/min. For the volatilization studies, samples of 500 mg (MWCNTs) and 0.21 and 1.59-1.60 g (green and sintered scraps, respectively) were placed in zirconia boats and heated at 5 (MWCNTs) or 4 °C/min (green and sintered scraps) to the oxidation temperature of 100-1,200 (MWCNTs) or 900 °C (green and sintered scraps) and maintained for 2 h. The air flow was 500 cm^3/min for all experiments. The oxidized products and powdered forms of the U_3O_8-C mixtures were observed using SEM (SU8230, Hitachi and AIS2100C, Seron Technologies, Uiwang-si, Republic of Korea, respectively).

RESULTS

1. Oxidation behavior of MWCNTs

The oxidation behavior of the MWCNTs in air was examined

Table 1. Specifications of Sintered scrap UC_2-C disk

Starting material	Diameter (mm)	Thickness (mm)	Density (g/cm^3)	Porosity (%)
UC_2-C	50	1.3	2.5	~70

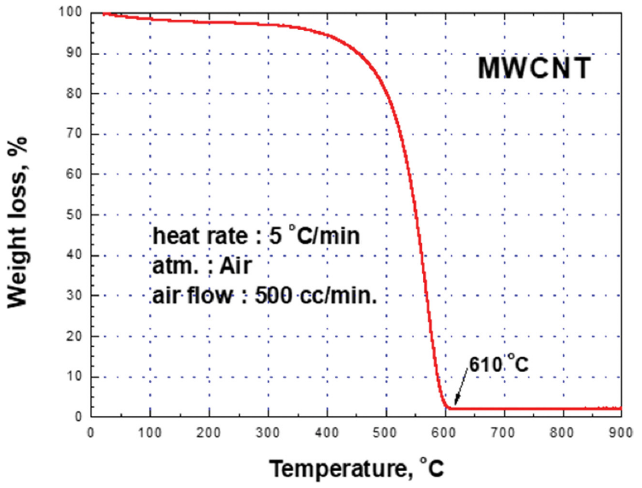

Fig. 4. TGA thermogram of MWCNTs.

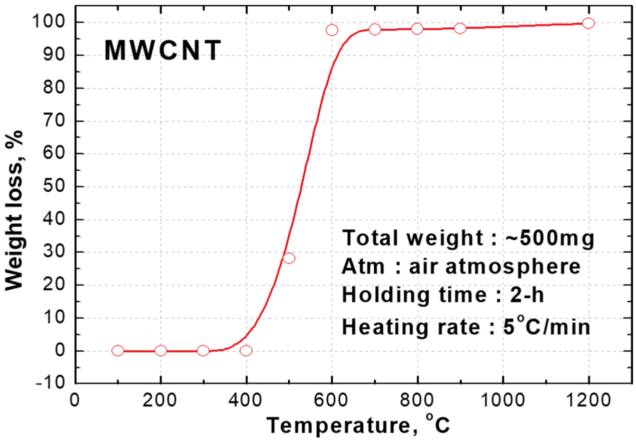

Fig. 5. Weight loss of MWCNTs at various oxidation temperatures.

using TG-DTA (Fig. 4). The weight gradually decreased until 400 °C, and then decreased drastically at ≥500 °C. At 610 °C, the MWCNTs were completely volatilized, except for a residual ~2 wt%, which likely comprises ash and other non-volatile materials. Contreras-Navarrete et al. [19] reported that, whereas MWCNTs maintain their structures until 400 °C when oxidized in air, their unique structures are lost at 500 °C or higher, with Fe impurities remaining as a residue.

Based on the TG-DTA results, we conducted volatilization studies in air at oxidization temperatures of 1,200 and 100-900 °C at intervals of 100 °C, using larger quantities of MWCNTs (~500 mg) and an electric furnace. Fig. 5 shows the weight loss of the MWCNTs at different oxidation temperatures. At ≥600 °C, the MWCNTs are completely volatilized. In summary, the volatilization behavior of MWCNTs depends on the oxidation temperature, regardless of the quantity of MWCNTs.

Fig. 6 shows the color changes of the MWCNTs relative to the oxidation temperature. At 500 °C, the black MWCNTs are partially volatilized with some red impurity particles observed. At 600 °C, the MWCNTs are mostly volatilized, with only a few black particles remaining along with the red impurity particles. At ≥700 °C, the MWCNTs are almost entirely volatilized, with the impurities turning completely red. The red residue is magnetic and thus is likely Fe.

Fig. 7 shows the changes in the MWCNT morphology with varying oxidation temperature. When the MWCNTs are oxidized at 500 °C (Fig. 7(e)), the morphologies resemble those of the untreated MWCNTs shown in Fig. 3. At 600 °C (Fig. 7(f)), the MWCNTs are almost completely volatilized, with some non-volatilized MWCNTs

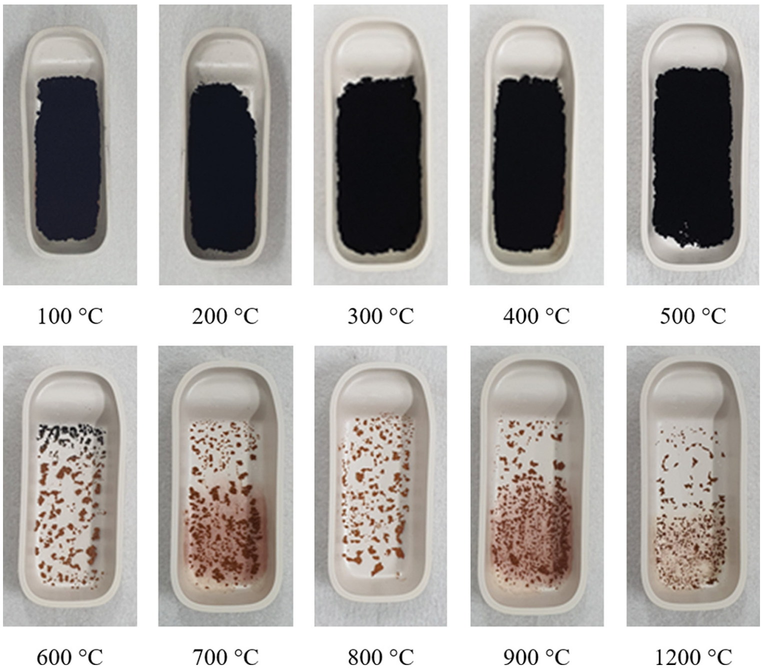

Fig. 6. Color changes of MWCNTs in zirconia boats relative to oxidation temperature.

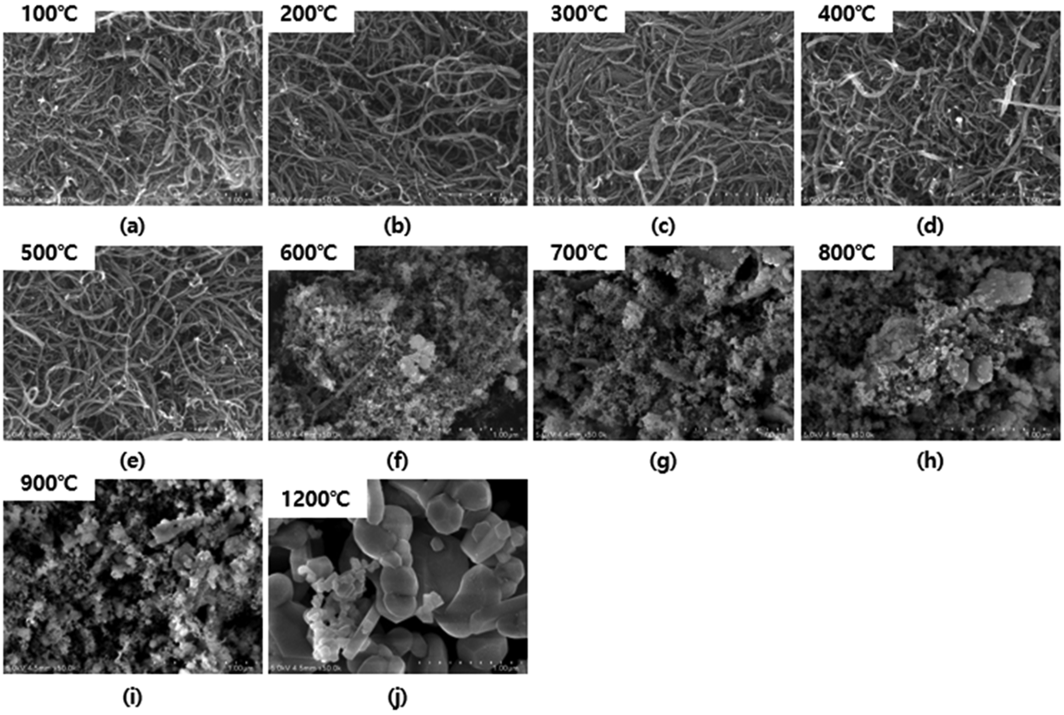

Fig. 7. Morphology of MWCNTs relative to oxidation temperature.

remaining along with some impurities. At 900 and 1,200 °C (Figs. 7(i) and (j), respectively), the MWCNTs are completely volatilized, and the sizes of the impurity particles are considerably increased with increasing temperature. The resulting crystalline grains were identified as Fe via energy dispersive X-ray spectroscopy. Thus, the MWCNTs contain mostly Fe impurities.

2. Oxidation behavior of Green Scrap

The oxidation behavior of the green scrap (U_3O_8 (70 wt%)-MWCNTs (30 wt%)) was examined using TG-DTA and volatilization studies. The mixture was prepared shortly prior to the studies. The SEM image shown in Fig. 8 reveals that the U_3O_8-C mixture comprises mixed U_3O_8 powder particles and MWCNTs.

For TG-DTA, a 30 mg sample of the U_3O_8-C mixture was used, and the results are shown in Fig. 9. To accurately determine the volatilization behavior at different temperatures, the weight loss of the U_3O_8 powder is noted. The TGA thermograms shown in Fig. 9 reveal that the weight loss of the U_3O_8-C mixture increases with temperature, and then plateaus at >560 °C at a weight loss of approximately 30%. This may be attributed to the additives and water in the sample volatilized during heating, in addition to the complete volatilization of the MWCNTs. Two exothermic peaks are observed at 280 and 510 °C in the DTA thermogram of the U_3O_8-C mixture. The peak at 280 °C is attributed to the volatilization of the bonding agent and dispersant, whereas the peak at 510 °C is attributed to the drastic volatilization of the MWCNTs, based on the altered morphologies of the MWCNTs at >500 °C shown in

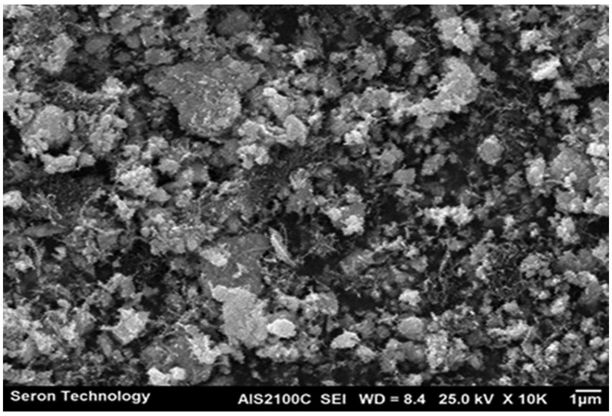

Fig. 8. U_3O_8-C mixture in powder form.

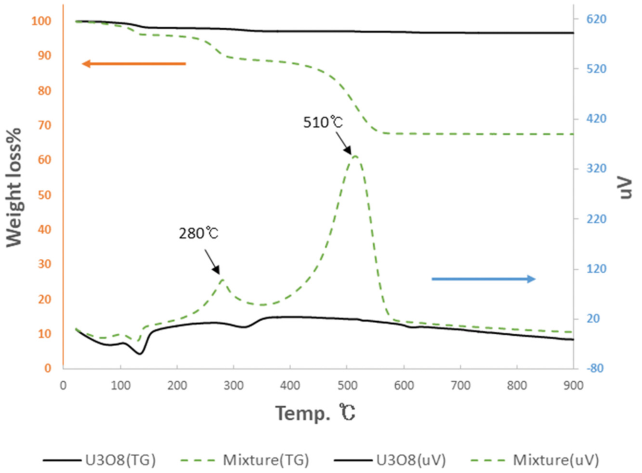

Fig. 9. TG-DTA thermograms of U_3O_8 and U_3O_8-C mixtures.

Table 2. Weight of UC_2-C fragment and powder before and after heating

Conditions	UC_2-C form	Weight (g)		Weight loss (%)
		Before heating	After heating	
Air	Fragment	1.59	1.34	15.7
900 °C, 2 h	Powder	1.60	1.31	18.1

Fig. 7.

Volatilization studies were performed in an electric furnace using a larger quantity of the U_3O_8-C mixture (0.21 g). The heating temperature of 900 °C was determined based on the MWCNT volatilization results. After sufficient cooling of the electric furnace, the content of the zirconia boat was re-weighed. The percent of weight loss was 28% based on the difference between the weight before and after heating. This is 2% less than the theoretical weight loss of 30%, which may be due to an increase in the impurity content during oxidation. Another cause may be the air not fully penetrating the mixture because of the higher weight of the specimen, resulting in partial volatilization of the MWCNTs. Therefore, to completely volatilize carbon in large quantities of scrap, along with a sufficient duration of heating, dispersion is recommended to facilitate a larger contact area between the powder and air.

3. Oxidation behavior of Sintered Scrap

During the carbothermal reduction of UC_2-C, the carbon is partially sublimated to CO or CO_2 and volatilized. Thus, the composition of the sintered disk is 80 wt% UC_2-20 wt% C [25]. Oxidation may convert this UC_2-C mixture to U_3O_8, assuming that the carbon is completely volatilized. Lau et al. [26] noted that to yield only U_3O_8, combustion should occur at 800 °C due to the presence of excess carbon in the form of graphite. Generally, if the UC_2 particles are large, the reaction with oxygen yields U_3O_8, with UO_2 as an intermediate product. However, if the powder particles are small, e.g., after pulverization, they may be immediately converted to U_3O_8, but this direct reaction may only occur if the carbon is completely volatilized.

The mechanism of oxidation consists of two stages.

Stage 1: $2UC_2\text{-}C+3O_2\rightarrow 2UC_2+CO+CO_2$
Stage 2: $3UC_2+8O_2\rightarrow U_3O_8+4CO+2CO_2$

In the first stage, the parent material C is oxidized and volatilized to CO and CO_2 in UC_2-C, and in the second stage, UC_2 is oxidized to form U_3O_8, during which CO and CO_2 are volatilized. Although the reaction time may affect this sequential reaction, the separation and confirmation of the two steps are challenging in high-temperature oxidation, and thus, the oxidation time was set to 2 h for the study. Generally, if the oxidation time is too short, there are some possibilities that complete oxidation to U_3O_8 will not occur in UC_2-C, and some carbon will remain. Furthermore, according to the results of the oxidation behavior of the MWCNTs and green scraps, the MWCNTs may be sufficiently volatilized at 700 °C or higher. However, the oxidation temperature was set to 900 °C to transfer sufficient thermal energy, because temperature differences may occur between the temperatures of the hot wire, measurement site, and transferred heat.

To examine the oxidation behavior of different forms of sintered scrap, two types of sintered scrap were prepared: fragmented and powdered. The powdered specimen was formed via pulverization for 10 min, whereas the fragmented specimen was broken into pieces. The oxidation temperature of 900 °C was selected based on the aforementioned conditions of the mixed powder process and Lau et al.'s findings [26]. The specimen size ranged from 1.59 (fragmented) to 1.60 g (powdered).

Table 2 shows the weight losses of the fragmented and powdered sintered specimens before and after heating. The heated powder exhibits a 2.4% higher weight loss (18.1%) than that of the heated fragments (15.7%). This is attributed to the difference in the specific surface areas of the fragmented and powdered specimens. The powdered form generally promotes a more efficient reaction because of its larger specific surface area. Therefore, pulverizing the specimen before heating is preferable. However, regardless of the specimen form, the percent of weight loss is smaller than the entire amount of volatilized carbon.

Fig. 10 shows images of the fragmented and powdered sintered disk specimens in zirconia boats. The fragments maintain their shapes during heating, and thus, the carbon is not fully volatilized rather than powdered form. Consequently, to increase the percent of weight loss, a different type of container (rectangular rather than a narrow cylinder) or pulverization should be used to facilitate more interactions with the reaction gas.

X-ray diffraction (XRD; MiniFlex, Rigaku, Japan) was used to comparatively analyze the U_3O_8 raw powder employed in target production and the heated scrap powder after thermal treatment to confirm whether the thermally treated powder was converted to U_3O_8. Fig. 11 shows the XRD patterns of the U_3O_8 raw powder (a) and the heated scrap powder (b), with identical peaks observed.

Additional studies were conducted to determine the percent of weight loss of heated scrap powder after H_2 reduction and confirm that the heated scrap powder obtained following thermal treatment was U_3O_8. The optimal weight loss was 3.8% when reducing U_3O_8 to UO_2 and may be calculated as follows. The atomic

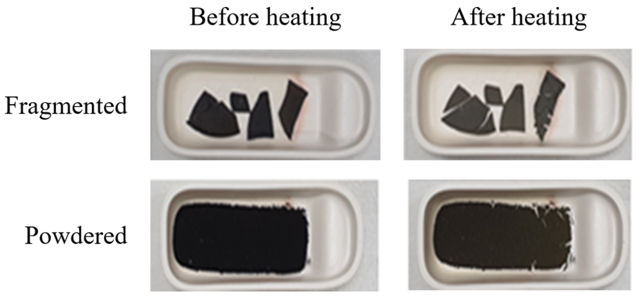

Fig. 10. Morphology of UC_2-C fragments and powder before and after heating under air at 900 °C for 2 h.

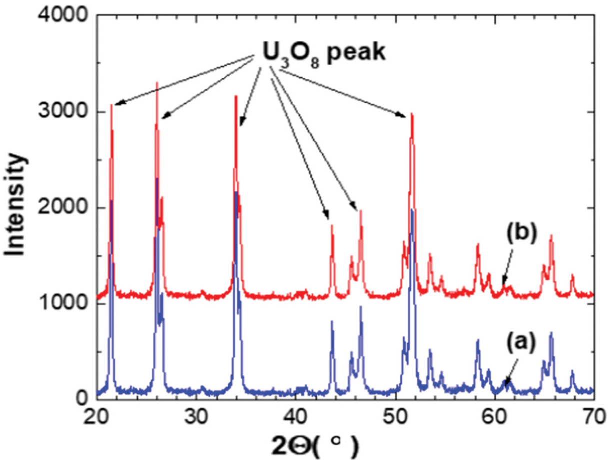

Fig. 11. XRD peaks of the U_3O_8 raw powder (a) and the heated scrap powder (b).

masses of U and O are defined as 238 and 16 g, respectively.

Reduction Formula: $U_3O_8 \rightarrow 3UO_2 + O_2(g)$
Theoretical Weight Loss (%)=

$$\frac{wt(U_3O_8) - wt(3UO_2)}{wt(U_3O_8)} \times 100 = \left(\frac{842-810}{842}\right) \times 100 = 3.8$$

The powder (4.285 g) was heated at 2 °C/min in an H_2 atmosphere after thermal treatment, reduced for 2 h at 900 °C, and then cooled to room temperature in the H_2 atmosphere to determine the weight loss (%). The final weight of the powder was 4.122 g.

Weight loss of powder (%)={(4.285−4.122)*100}/(4.285)=3.8

Therefore, the oxidized powder is mostly converted to U_3O_8 even when a minimum amount of impurities remains from MWCNT residue or the carbon components that have not been removed depending on the type of UC_2-C scrap.

CONCLUSIONS

To recover uranium from scrap generated during the fabrication of UC_2-C disks for use as a heavy ion accelerator target material, we conducted carbon volatilization studies at varying temperatures under air and obtained the following results:

1) At approximately 600 °C, the MWCNTs were almost completely volatilized.

2) The weight loss of the U_3O_8-MWCNT mixed powders decreased at varying temperatures, displaying a similar pattern to that of the weights of the MWCNTs. This was likely because the mixtures were homogeneous.

3) To increase the rate of UC_2-C weight loss in response to oxidation, pulverization was more effective than fragmentation.

4) To oxidize UC_2-C disks, pulverization to form a powder is recommended.

ACKNOWLEDGEMENTS

This study was supported by the Rare Isotope Accelerator Development Project through the Ministry of Science and ICT, National Research Foundation of Korea, and Institute for Basic Science (Study Number: NRF-2019-M7A1A1-032994).

REFERENCES

1. C. Gasparrini, R. Podor, D. Horlait, M. J. D. Rushton, O. Fiquet and W. E. Lee, *J. Nucl. Mater.*, **494**, 127 (2017).
2. B. M. Ma, *Nuclear reactor materials and applications*, Van Nostrand Reinhold, New York (1983).
3. F. Le Guyadec, C. Rado, J. Joffre, S. Coullomb, C. Chatillon and E. Blanquet, *J. Nucl. Mater.*, **393**, 333 (2009).
4. K. A. Peakall and J. E. Antill, *J. Less-Common Met.*, **4**, 426 (1962).
5. K. Naito, N. Kamegashira, T. Kondo and S. Takeda, *J. Nucl. Sci. Technol.*, **13**, 260 (1976).
6. D. Scarpa, L. Biasetto, S. Corradetti, M. Manzolaro, A. Andrighetto, S. Carturan, G. Prete, P. Zanonato and D. W. Stracener, *Eur. Phys. J. A*, **47**, 32 (2011).
7. J. P. Ramos, *Nucl. Instrum. Methods Phys. Res. B*, **463**, 201 (2020).
8. B. Hy, N. Barré-Boscher, A. Özgümüs, B. Roussière, S. Tusseau-Nenez, C. Lau, M. Cheikh Mhamed, M. Raynaud, A. Said, K. Kolos, E. Cottereau, S. Essabaa, O. Tougait and M. Pasturel, *Nucl. Instrum. Methods Phys. Res. B*, **288**, 34 (2012).
9. A. Andrighetto, L. Biasetto, M. Manzolaro, M. Barbui, G. Bisoffi, S. Carturan, M. Cinausero, F. Gramegna, G. Prete, V. Rizzi, C. Antonucci, S. Cevolani, C. Petrovich, P. Colombo, G. Meneghetti, P. Di Bernardo, P. Zanonato, I. Cristofolini, V. Fontanari, B. Monelli and R. Oboe, *Nucl. Instrum. Methods Phys. Res. B*, **266**, 4257 (2008).
10. S. Corradetti, A. Andrighetto, M. Manzolaro, D. Scarpa, J. Vasquez, M. Rossignoli, A. Monetti, M. Calderolla and G. Prete, *EPJ Web Conf.*, **66**, 11009 (2014).
11. S. Carturan, M. Tonezzer, L. Piga, P. Zanonato, P. Colombo, A. Andrighetto, L. Biasetto, P. Di Bernardo, G. Maggioni, F. Gramegna and G. Prete, *Nucl. Instrum. Methods Phys. Res. A*, **583**, 256 (2007).
12. Y. Zhang and G. D. Alton, *Nucl. Instrum. Methods Phys. Res. A*, **521**, 72 (2004).
13. L. Biasetto, P. Zanonato, S. Carturan, P. Di Bernardo, P. Colombo, A. Andrighetto and G. Prete, *J. Nucl. Mater.*, **404**, 68 (2010).
14. M. J. Joung, J. W. Jeong, W. Hwang, S. G. Hong, J. Y. Kim, S. J. Park, H. J. Woo, B. H. Kang and S. H. Na, *Nucl. Instrum. Methods Phys. Res. B*, **456**, 97 (2019).
15. A. Monetti, R. A. Bark, A. Andrighetto, P. Beukes, J. L. Conradie, S. Corradetti, D. Fourie, C. Lussi, M. Manzolaro, G. Meneghetti, G. Prete, M. Rossignoli, D. Scarpa, P. Van Schalkwyk, N. Stoddart and J. Vasquez, *Eur. Phys. J. A*, **52**, 168 (2016).
16. A. Monetti, A. Andrighetto, C. Petrovich, M. Manzolaro, S. Corradetti, D. Scarpa, F. Rossetto, F. M. Dominguez, J. Vasquez, M. Rossignoli, M. Calderolla, R. Silingardi, A. Mozzi, F. Borgna, G. Vivian, E. Boratto, M. Ballan, G. Prete and G. Meneghetti, *Eur. Phys. J. A*, **51**, 128 (2015).
17. Environment Agency Interim Advice on Wastes Containing Unbound Carbon Nanotubes (May 2008). Available from https://nanotech.law.asu.edu/Documents/2009/08/nano-waste_199_5154.pdf.
18. S. P. B. Sousa, T. Peixoto, R. M. Santos, A. Lopes, M. d. C. Paiva and A. T. Marques, *J. Compos. Sci.*, **4**, 106 (2020).

19. J. J. Contreras-Navarrete, F. G. Granados-Martínez, L. Domratcheva-Lvova, N. Flores-Ramírez, M. R. Cisneros-Magaña, L. García-González, L. Zamora-Peredo and M. L. Mondragón-Sánchez, *Superficies y Vacío*, **28**, 111 (2015).
20. C. Gasparrini, R. Podor, O. Fiquet, D. Horlait, S. May, M. R. Wenman and W. E. Lee, *Corros. Sci.*, **151**, 44 (2019).
21. S. K. Mukerjee, G. A. Rama Rao, J. V. Dehadraya, V. N. Vaidya, V. Venugopal and D. D. Sood, *J. Nucl. Mater.*, **210**, 97 (1994).
22. H. J. Borchardt, *J. Inorg. Nucl. Chem.*, **12**, 113 (1959).
23. R. M. Dell and V. J. Wheeler, *J. Nucl. Mater.*, **21**, 328 (1967).
24. B. H. Jo, Y. H. Shim, B. H. Kang and J. W. Jung, South Korea Patent, 10-2235855 (2021).
25. L. Biasetto, S. Corradetti, S. Carturan, R. Eloirdi, P. Amador-Celdran, D. Staicu, O. Dieste Blanco and A. Andrighetto, *Sci. Rep.*, **8**, 8272 (2018).
26. C. Lau, B. Roussière, D. Verney, O. Bajeat, F. Ibrahim, F. Clapier, E. Cottereau, C. Donzaud, M. Ducourtieux, S. Essabaa, D. Guillemaud-Mueller, F. Hosni, H. Lefort, F. Le Blanc, A. C. Mueller, J. Obert, N. Pauwels, J. C. Potier, F. Pougheon, J. Proust, J. Sauvage and A. Wojtasiewicz, *Nucl. Instrum. Methods Phys. Res. B*, **204**, 246 (2003).